INVESTIGATING THE SEISMIC AND GEOLOGICAL STRUCTURE OF THE MARTIAN CRUST AT THE DICHOTOMY BOUNDARY. B. Tauzin[1,2], L. Pan[1], C. Michaut[1], C. Quantin[1], N. Schmerr[3], C. Perrin[4], P. Lognonné[4], and V. Ansan[5] [1]Université de Lyon, UCBL, ENS Lyon, CNRS, Laboratoire de Géologie de Lyon, Terre, Planètes, Environnement (2 rue Raphaël Dubois, Villeurbanne, 69622, France). [2]Research School of Earth Sciences, Australian National University, (Australian Capital Territory 0200, Canberra, Australia). [3]University of Maryland, Department of Geology, (College Park, Maryland 20742, U.S.A.). [4]Institut de Physique du Globe de Paris, Univ Paris Diderot-Sorbonne Paris Cité, (Paris Cedex 13, France). [5]Université de Nantes, Laboratoire de Planétologie et Géodynamique, (44322 Nantes Cedex 3). (benoit.tauzin@univ-lyon1.fr).

Introduction: We present investigations on the regional geologic context of the InSight landing site, and the adjacent Elysium Mons and southern Highlands. We use multiple orbital analyses of rock exposures in the craters and local scarps to build a regional geological model. This *a priori* structure is used to model the seismic response expected from the SP and VBB instruments of the SEIS experiment (Seismic Experiment for Interior Structures) on board InSight lander [1, 2]. We focus on the response recorded in the coda of teleseismic P-waves, and on the crustal-guided seismic wavefield. We discuss the potential of the seismic data to gain a wide view of the crustal structure and geologic history of the vicinity of the InSight landing site.

The Martian crust at the dichotomy boundary: The InSight landing site is situated between the Elysium volcanic structure and the dichotomy boundary (Fig. 1A) [3]. The region has been shaped by the early formation and subsequent modification of the Martian dichotomy [4, 5]. InSight landed within an Early Hesperian unit with wrinkle ridges inferred to be volcanic in origin [6-9], which is also adjacent to the Medusae Fossae Formation.

Orbital data, methods: We study the high-resolution images covering the broad region of the landing site (125°E to 145°E, 2°S to 15°N), in particular outcrops in impact craters and local scarps. The datasets include CRISM (Compact Reconnaissance Imaging Spectrometer for Mars) targeted images (18-36 m/pixel, 438 channels) following previous processing method [10], as well as HiRISE (High Resolution Imaging Science Experiment) and CTX (Context Camera) images. We build a geological cross-section across the landing site from orbital analysis of the limited rock exposures in the craters and local scarps in the region (Fig. 1).

Orbital data, detections: We detected olivine spectral signatures on small craters rims close to the InSight landing site, on the ridged plains unit (Fig. 1). We also identified absorptions related to Fe/Mg phyllosilicate in the 50-km Kalpin crater on the southwest flank of Elysium Mons. Other than the spectral signature, the central peak of Kalpin crater shows layered, cliff-bench morphology, consistent with outcrops of sedimentary rocks on Mars [11]. Though the exposure is limited, it is possible that such a unit is more extensive within the subsurface of Elysium Planitia. Other large craters in the landing site vicinity also show possible detections of hydrated minerals, but the absorptions are obscured. This analysis suggests diverse lithologies underlie the lava flows unit, in which InSight landed. In particular, the clay-bearing altered deposit and Medusae Fossae Formation-like sedimentary unit are potential analogs for the subsurface crust (Fig. 1B).

Seismic data, methods: We predict the seismic response of the inferred shallow geological structure. We use a 40 m profile for the regolith derived previously [12], and apply seismic velocities (v_p and v_s) from Earth analogue rocks, interpolating the elastic proper-

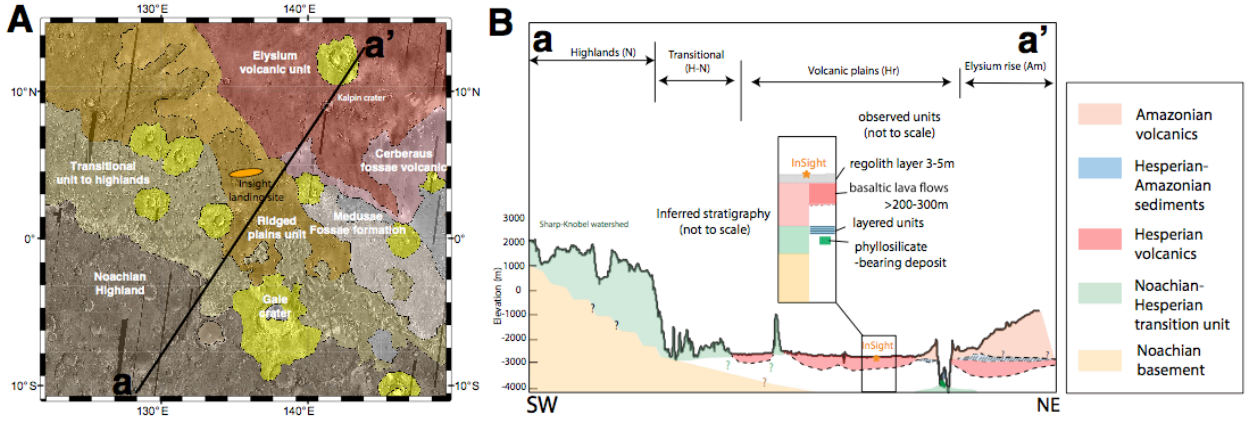

Figure 1: A. Geological map of the InSight landing site vicinity based on [6], with major geological units labeled. Kalpin crater on the a-a' profile is the location of the phyllosilicate detection. B. A schematic cross-section of the InSight landing site across the dichotomy boundary with possible subunits within the crust (from Pan & Quantin 2018). A stratigraphic column is shown for the landing site region with units delineated within the subsurface based on the observations of exposures in central peaks of impact craters.

ties between the different layers. Since the depth, elastic and attenuation properties of the transition in the basaltic layer are uncertain; we varied these parameters in a suite of models. The calculation of synthetic seismograms is based on numerical integration of the plane wave reflection coefficient for a stack of homogeneous layers [13, 14]. Calculations are done up to 50 Hz for simple receiver-side stratifications, and up to ~12 Hz for a "full" wavefield propagation from the teleseismic source. *A priori* geological models combining a regolith and a weak zone generate high-frequency crustal-guided waves.

Seismic modeling, results: The regolith generates a monochromatic teleseismic P-wave coda with a large resonance peak at ~7 Hz (Fig. 2B, D). This response is modulated by the response of the underlying crust, which superimposes small amplitude and narrower peaks (Fig. 2B, D). Later in the seismograms (Fig. 2C), the combination of a regolith and a weak layer generates long-duration, strong amplitude, wave-packets recorded with time linearly increasing with distance. These are Pn waves guided in near surface layering [15, 16].

Discussion and conclusions: Pn waves share similar spectral resonance peaks with the P-wave coda. The peak frequencies, amplitudes, and widths are related to the crustal properties, including anelastic attenuation [15]. If shallow weak zones are distributed over large regions of Elysium Mons and of the adjacent Highlands, a fine analysis of the crustal-guided wavefield will provide large-scale constraints on the shallow crust. We will engage in theoretical and modeling efforts to further understand the character of this guided wavefield, in view of a comparison with the SEIS data.

Acknowledgement: This project has received funding from CNES, the European Union's Horizon 2020 research and innovation programme under the Marie Sklodowska-Curie grants agreement No. 751164 and No. 793824.

References: [1] Banerdt W. B. et al. (2017) LPS XLVIII Abstract #1896. [2] Lognnoné P. et al. (2018) *42 COSPAR Sci. Assembly*. B4.1-29-18. [3] Golombek M., et al. (2017) *Space Sci. Rev.* 211, 1-4, 5-95. [4] Tanaka K. L., Chapman M. G. and Scott D. H. (1992) *USGS* No. 2147. [5] Tanaka K. L. et al. (2014) *Planet. Space Sci* 95, 11-24. [6] Head J. W., Kreslavsky M. A. and Pratt S. (2002) *JGR Planets* 107, E1. [7] Salvatore M. R. *et al.* (2010). *JGR Planets*, 115(E7). [8] Ody, A. *et al.* (2013) *JGR Planets* 118, 2: 234-262. [9] Golombek et al. (2018) *Space Sci.* Rev., 214(5), 84. [10] Pan et al. (2017) *JGR Planets*, 122, 9, 1824-1854. [11] Malin, M. C. and Edgett K. S. (2000) *Science* 290, 5498, 1927-1937. [12] Knapmeyer-Endrun, B. et al., (2018) *Space Sci. Rev.*, 214(5), 94. [13] Fuchs K. & Muller G. (1971) *Geophys. J.R. Astron. Soc.*, 23, 417–433. [14] Randall G.E. (1989) *Geophys. J. Int.*, 99, 469-481. [15] Sereno T. and Orcutt J. (1985) *J. Geophys. Res.*, 90, 12,755-12,776. [16] Kennett B.L.N. and Furumura T. (2013) *Geophys. J. Int.*, 195, 1862-1877.

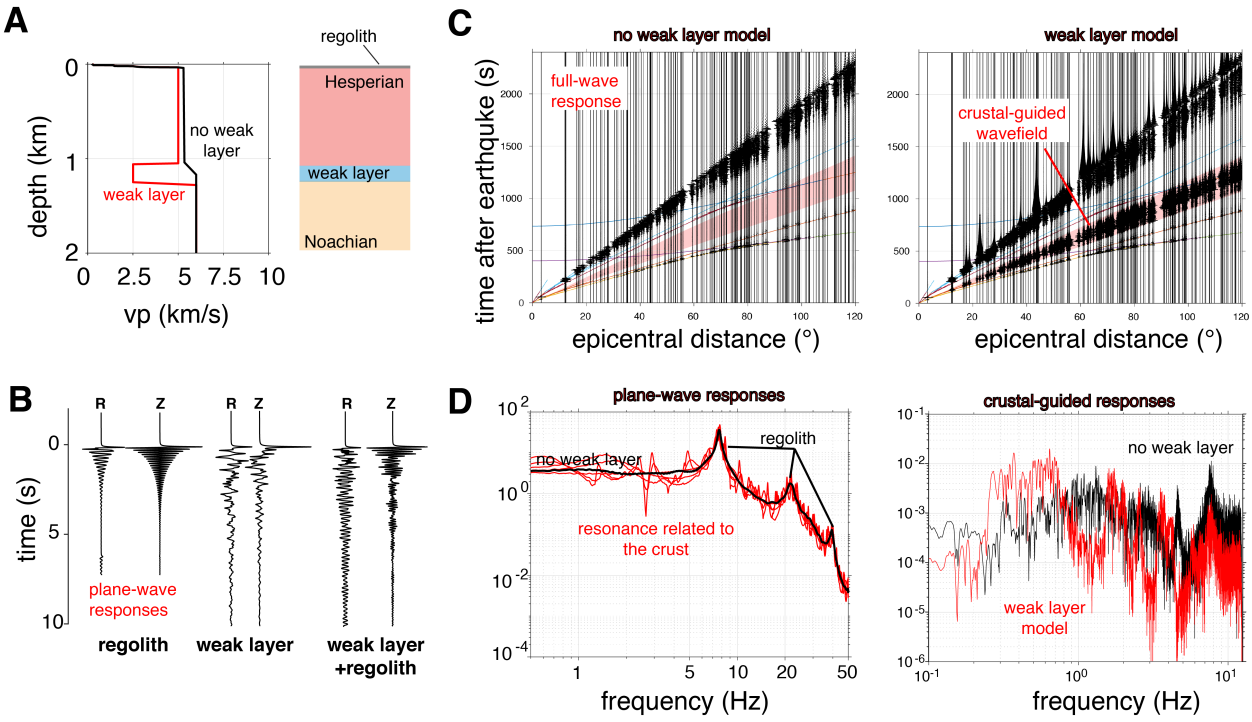

Figure 2: A. Tested geological models. B. Vertical (Z) and radial (R) responses recorded in the P-wave coda due to excitation by a teleseismic plane wave. The responses are shown for the regolith alone, the crust alone, and the combination of the two. C. Full-wavefield responses for the two models shown in (A). When a weak zone is present, these responses show a wave-packet associated with Pn crustal-guided waves (highlighted in red). D. Responses in the frequency domain for the P-wave coda (left) and the crustal guided wavefield. The spectra (black and red) are associated with the models in (A).